J. Fluid Mech. (1971), *vol.* 50, *part* 3, *pp.* 431–448
Printed in Great Britain

Degeneration of resonantly-excited standing internal gravity waves

By A. D. McEWAN

C.S.I.R.O., Division of Meteorological Physics,
Aspendale, Victoria, 3195 Australia

(Received 24 June 1970 and in revised form 24 June 1971)

The factors bringing about the irreversible distortion or degeneration of a continuously forced standing internal gravity wave in a linearly stratified fluid are studied experimentally and theoretically. For a rectangular container there is strong evidence that the process is initiated by the unstable growth, from a subliminal level, of free wave modes forming triads in second-order resonant interaction with the original wave. These free modes grow by de-energizing the original wave and may collectively induce kinematical conditions sufficiently severe to create localized regions of density discontinuity within the fluid, leading to turbulence.

Although the possible free wave modes are doubly infinite in number, the geometrical constraints greatly reduce the number of possibilities for resonant triads. In many cases this permits critical wave amplitude to be predicted by consideration of one triad only, and the results are in excellent agreement with experiment.

It is speculated that a closely similar process explains observations by Malkus (1968), Aldridge & Toomre (1969), and McEwan (1970) in the analogous context of inertial oscillation of contained rotating fluids.

1. Introduction

Energy absorption and dissipation by means of internal gravity waves is increasingly recognized as being an important influence in the large-scale distribution of momentum and heat in the ocean and the atmosphere, but although a large body of literature has accumulated on the behaviour of such waves at small amplitudes, the kinematical details of how they deform at large amplitudes and become effective in energy dissipation is far from complete.

The present study is part of a programme directed at filling in some of these details for continuously stratified media in which the motion is partly or completely wave induced. It concerns the evolution of a standing internal gravity wave fully bounded within a rectangular container, when continuously forced near resonance.

The only previously published work along similar lines was by Thorpe (1968) who found that if the forcing was strong enough localized 'turbulence' occurred. This, he associated with shear across internal wave rays originating at the wave makers. No limitation on possible wave amplitudes was established and the cross modes which characterize the 'breaking' of surface standing waves (Taylor 1953)

were not observed although the presence was noted of waves of frequency unequal to the forcing frequency.

For the present study a trial experiment was performed in which a standing wave in weak linearly stratified salt solution was continuously forced to gradually increasing amplitude. Above a specific amplitude the wave became progressively distorted, but unless the forcing was particularly violent the process was orderly and repeatable. In all cases the creation of true turbulence was preceded by the occurrence of localized regions of strongly intensified density gradient, and this in turn was, with one exception, preceded by the visible emergence of other free wave modes bearing individually no simple relation to the original. Even when the wave pattern was severely distorted an obvious symmetry or antisymmetry was conserved, and in some cases the modulating waves became dominant over the original without turbulence appearing at any time.

In this paper a theory is developed and convincingly verified explaining the initial stages of the degeneration process as being an unstable resonant wave interaction in which a pair of free wave modes are selectively amplified from a subliminal (noise) level, each energized by the interaction of the other with the original forced wave. Viscosity acts to dissipate the transferred energy; so there exists for a given forced wave a critical amplitude below which degeneration does not occur.

For travelling-wave systems, the theory of resonant interaction has been thoroughly explored. Among the analyses more closely relevant to the present case are those by Thorpe (1966) and Simmons (unpublished work, see Martin, Simmons & Wunch (1969)) for internal waves in continuous stratification. The interaction between a forced pair of travelling internal waves has been demonstrated experimentally by Martin *et al.* (1969). Mutual interaction mechanisms similar to the present one have been proposed to explain the progressive distortion of surface waves (Benjamin & Fier 1967) and internal waves on a diffuse interface between miscible fluids (Davis & Acrivos 1967). Craik (1968) noted the existence of a strong interaction exciting oblique waves from a travelling surface wave in a shear flow. McGoldrick (1970) demonstrated the unstable interaction of a suitably tuned capillary-gravity wave with its own second harmonic, under the action of viscous damping.

For the purpose of quantitatively verifying the theoretical analysis, the present experiment shares with McGoldrick's the benefit of well-defined interaction modes, but permits viscous dissipation to be estimated with greater accuracy. To reveal internal gravity wave interaction the standing-wave configuration possesses distinct advantages, in simplicity and unambiguity of measurement, over travelling-wave configurations. Indeed it offers promise of considerable fruitful theoretical and experimental exploration, although for the present study interest was necessarily confined to the initial stages of interaction, when the unstable modes are weak.

The selective mutual interaction demonstrated here may well be, within the constraints of viscosity, an ubiquitous feature in the dynamical behaviour of waves, particularly when the motion is bounded. One case in point bearing a dynamical resemblance to the present one, and exhibiting a close correspondence in the evolution of the instability, is that of inertial oscillations in a uniformly-

rotating closed container. No detailed analysis has yet been made but an examination (not given here) of orders of magnitude in the experiments of Malkus (1968), Aldridge & Toomre (1969) and McEwan (1970) shows consistency with a similar interaction mechanism.

2. Analysis

2.1. *First-order resonant solution for a standing wave*

Liquid with density $\rho(z)$ and an undisturbed weak linear density gradient $d\rho/dz = \rho_0'$ completely fills a rectangular container of height H, length L and breadth B. Co-ordinates x and y are in the length and width directions, and originate at the centre plane on one lower corner of the tank.

The end wall remote from the origin comprises a plane paddle oscillating sinusoidally at frequency ω through a small angle 2α about an axis $(L, y, \frac{1}{2}H)$. In its mean position the paddle occupies the plane $x = L$.

With the Boussinesq approximation the equations for motion in the x, z plane may be written

$$\left.\begin{aligned} (\nabla^2\psi)_t + J(\nabla^2\psi, \psi) &= g\rho_x/\rho, \\ \left\{\psi_z \frac{\partial}{\partial x} - \psi_x \frac{\partial}{\partial z} + \frac{\partial}{\partial t}\right\}\rho &= 0, \end{aligned}\right\} \tag{1}$$

where $\psi_z = u$, $-\psi_x = w$, the horizontal and vertical components of motion, J is the Jacobian determinant, and g is gravitational acceleration. Density is expressed as:

$$\left.\begin{aligned} \rho &= \rho_0(0) + z\rho_0' + \Sigma\rho_j(x, z, t) \\ \text{and} \quad \psi &= \Sigma\psi_j = \Sigma A_j s_j(x, z, t). \end{aligned}\right\} \tag{2}$$

A_j is the amplitude of an individual mode j in units of stream function.

Combining equations (1), to first order in amplitude

$$(\nabla^2\psi)_{tt} + \Omega^2\psi_{xx} = 0, \tag{3}$$

where $\Omega = (-\rho_0' g/\rho_0(0))^{\frac{1}{2}}$, the buoyancy frequency. Consider now the initial stages of motion when paddle oscillation is started.

For

$$\left.\begin{aligned} &t > 0, \\ &\psi_x = 0 \quad \text{at} \quad z = 0, H, \\ &\psi_z = \begin{cases} \sum\limits_N a_N \cos(N\pi z/H) \sin\omega t, & \text{at} \quad x = L, \\ 0, & \text{at} \quad x = 0. \end{cases} \end{aligned}\right\} \tag{4}$$

where a_N is defined by the triangular displacement of the paddle:

$$a_N = \begin{cases} 0 & N \text{ even} \\ -4\alpha\omega H/(\pi^2 N^2), & N \text{ odd}. \end{cases}$$

By a Laplace transform treatment roughly equivalent to that of Baines (1967) equations (3) and (4) give the following resonantly forced modes,

$$\psi(x, z, t) = \sum_N (-1)^M \frac{a_N n}{m^3 L} \cdot \frac{\omega^2}{\Omega^2} \cdot \sin(nz) \{\cos(\omega t) \sin(mx) \cdot (\omega t - (-1)^M m^3 L \Omega^2 n^{-2} \omega^{-2}) + \sin(\omega t) \cdot (x m^3 \Omega^2 n^{-2} \omega^{-2} \cos(mx) - \tfrac{1}{2} \sin(mx))\}. \tag{5}$$

For resonance (assumed in deriving the above expression) the forcing frequency must be such that the dispersion relation

$$n^2/m^2 = (\Omega^2 - \omega^2)/\omega^2 \tag{6}$$

is satisfied, wherein the horizontal and vertical wave-numbers m and n are prescribed by the boundary conditions to repeat the streamline pattern M times in the horizontal length L and N times in the vertical height H. Thus $m = M\pi/L$, $n = N\pi/H$; M and N are integers. Through (6), m is defined by N and the series in (5) is absolutely convergent like N^{-3}.

The initial rate of growth in amplitude of an individual member ψ_j of such a resonant set is then

$$dA_j/dt = \omega_j b_j,$$

where
$$b_j = (-1)^{M_j} a_N n_j \omega_j^2 / L m_j^3 \Omega^2 \tag{7}$$

and
$$\psi_j = A_j s_j, \quad s_j = \sin mx \sin nz \cos \omega t. \tag{8}$$

2.2. *Viscous dissipation and terminal amplitude*

To calculate the terminal amplitude of a steadily forced standing wave in a liquid of low viscosity, an energy integral approach is used, for reasons which will become apparent.

Near to the container boundaries motion is nearly tangential and dominated by viscous stress. Provided the dimensionless amplitude $A/\omega H^2$ is small enough and boundary layers are sufficiently thin, tangential gradients can be neglected and vertical and horizontal motion equations simplify to

$$\left.\begin{aligned} (u_i - u)_t + \nu u_{\gamma\gamma} &= 0, \\ (w_i - w)_{tt} + \nu w_{\gamma\gamma t} - \Omega^2 (w_i - w) &= 0, \dagger \end{aligned}\right\} \tag{9}$$

where subscript i denotes interior motion. γ is the surface normal co-ordinate. Effects of salt diffusivity are neglected.

The solutions, subject to the boundary conditions

$$u(0) = w(0) = 0,$$

$$u(\gamma \to \infty) \to u_i \equiv U \cos \omega t,$$

$$w(\gamma \to \infty) \to W_i \equiv W \cos \omega t,$$

are
$$u = U_i(\cos \omega t - e^{-\eta} \cos(\omega t - \eta)) \Big\}$$
and
$$w = W_i(\cos \omega t + \epsilon e^{-\xi} \cos(\omega t + d\xi)), \Big\} \tag{10}$$

where
$$\eta = \gamma R^{\frac{1}{2}} / 2^{\frac{1}{2}} H,$$
$$\xi = \gamma R^{\frac{1}{2}} |\Omega^2/\omega^2 - 1|^{\frac{1}{2}} / 2^{\frac{1}{2}} H$$

and
$$\epsilon = \pm 1, \ \Omega \gtrless \omega.$$

R is a dissipation parameter, defined by

$$R = \omega H^2 / \nu. \tag{11}$$

† I am indebted to M. McIntyre and J. Hart for pointing out the importance of stratification in this equation.

Stratification does not alter the horizontal velocity profile, but changes the scale of the vertical velocity profile, for an external free wave motion, by a factor equal to the ratio of horizontal to vertical wave-number. Dissipation per unit area through the boundary layer is

$$\mu \int_0^\infty (u_\gamma^2 + w_\gamma^2)\, d\gamma.$$

Average level in time is

$$\rho\omega H(u_i^2 + n w_i^2/m)/2.2\tfrac{1}{2}R.$$

Using the inviscid free-mode description (8) to define $u_i, w_i(x, z)$, the mean energy dissipation rate within the boundary layers due to an individual mode j is

$$C_j = \frac{\rho H A_j^2 \omega}{4.2\tfrac{1}{2}R^{\frac{1}{2}}}(HL(mn+n^2) + 2BHm + n2n^2BL)_j. \tag{12}$$

Equation (8) is used also to approximate the internal field under the influence of viscosity. Integration of the complete dissipation function over the container volume and time averaging gives, for the internal dissipation rate I_j,

$$I_j = \frac{\rho A_j^2 \omega BLH^2}{8R}(m^2+n^2)_j^2 \tag{13}$$

to first order.

The inviscid growth rate (7) defines the rate at which a wave orthogonal in phase to the paddle acquires its energy. To find the terminal amplitude of a damped wave this rate is equated to the total mean dissipation rate. The energy in an individual mode of free oscillation $\psi_j = A_j s_j$ is

$$E_j = \tfrac{1}{2}\rho \int_\gamma ((\partial s/\partial x)^2 + (\partial s/\partial z)^2) A_j\, dV,$$

or, with (8),

$$E_j = \tfrac{1}{8}\rho A_j^2 BLH(m^2+n^2)_j. \tag{14}$$

We define a gross dissipation function G_j which includes the above dissipation terms and any others, say P_j, arising under specific experimental conditions, i.e.

$$G_j = (C+I+P)_j/\rho A_j^2 \omega_j H.$$

Now the interior motion of a resonant standing wave is defined to second order in amplitude (Thorpe 1968) and to order $R^{-\frac{1}{2}}$ by the inviscid form

$$\psi = A \sin mx \sin nz \sin(\omega t + \phi), \tag{15}$$

where ϕ is phase relative to paddle displacement.

If both forcing and dissipation are weak, equations (7) and (12) to (15) may be combined in the form of an energetic balance, to give for the variation in amplitude of a wave forced near resonance

$$dA/dt = \omega b \sin\phi - TA/(m^2+n^2), \tag{16}$$

where T is defined as $4\omega G/BL$. Using this formulation the terminal amplitude $A_T = \omega b \sin\phi (m^2+n^2)/T$ under continuous forcing, and decay rate without forcing ($b = 0$), may be determined.

If there exist together a number of small-amplitude free modes of the form of (15), their orthogonality guarantees that, within the order of the approximations made, each may grow and decay independently of the others. For a given fundamental mode amplitude A_1,

$$H_N = N^2 H_1, \quad I_N = N^4 I_1 \tag{17}$$

and $A_{T_N} = N^{-2} A_{T_1} G_1/G_N$ for a given phase where $N = 1, 3, 5$, etc., is the vertical modal number.

Normally the contribution of the highest harmonic modes to the net observed motion will be small. For the present case, only 'odd' resonant modes at equal frequency are forced by the paddle, and with $L/H = 3{\cdot}58$, $B/H = 0{\cdot}7$ $\omega/\Omega = 0{\cdot}488$, $R = 6{\cdot}8 \times 10^4$, the increase in measured terminal amplitude at $(\frac{3}{4}L, \frac{1}{2}B, \frac{11}{12}H)$ is 2·5 %. It is noteworthy that on a laboratory scale internal dissipation becomes comparable with wall dissipation for N of order 10.

2.3. *Resonant interaction*

If it is supposed that the motion is composed of a number λ of elements ψ_j, equations (1) might be combined in the form:

$$\sum^{j=\lambda} ([\nabla^2\psi]_{tt} + \Omega^2\psi_{xx})_j = \sum_{k,l}^{k,l=\lambda} \left\{ \frac{g}{H} J(\psi_k, \rho_l)_x - J(\nabla^2\psi_k, \psi_l)_t \right\} + \Sigma \text{ higher order terms.} \tag{18}$$

The homogeneous solution of this equation admits free modes of the form (15), whose frequency and spatial wave-number ratio are related by (6). Thorpe used a similar form with $k = l$ to deduce the finite-amplitude distortions to a standing internal wave. The first summation on the right-hand side constitutes the forcing of individual modes j by the second-order interaction of pairs of other modes k and l.

If the modes forced do not satisfy the dispersion equation (6), their amplitude will be defined by the interaction product of the forcing components on the right hand. However, if the periodicity in space and time required by (6) is reproduced by a pair of interacting free modes a third individual *free* mode may be resonantly forced by the interaction. Denoting ψ_1, ψ_2 and ψ_3 as such an interacting triad the conditions for second-order resonant interaction are then

$$\left.\begin{aligned} M_2 &= \pm M_1 \pm M_3, \\ N_2 &= \pm N_1 \pm N_3, \\ \omega_2 &= \pm \omega_1 \pm \omega_3, \quad (|\omega_j| \leqslant \Omega), \\ \text{and} \qquad (NL/MH)_j^2 &= (\Omega^2 - \omega^2)/\omega^2 \quad (j = 1, 2, 3), \end{aligned}\right\} \tag{19}$$

where M and N, as defined after (6) are horizontal and vertical modal numbers. Thus though the possible free modes are doubly infinite in number, there exists at most a singly infinite set of discrete values of L/H for which this kind of interaction is possible.

In the present context only one free mode ψ (and its harmonics) is forced externally. Other free modes must exist at a subliminal (noise) level but can only grow in pairs ψ_2, ψ_3 by interaction; a single mode could not grow in isolation since (6) would then be violated by the requirement that wave-numbers in all dimensions be half those of the main mode.

For a given L/H the interacting triads most closely satisfying (19) can be identified unambiguously by graphical methods. It is found (see table 1, §3.2) that two or more triads containing the forced main mode may be *close* to satisfying these equations, but for the present it is presumed that all interacting triads satisfying the equations exactly possess unique and *different* values of L/H. Attention is confined here to these specific geometries.

We nominate ψ_1 as the initial forced resonant mode and ψ_2 and ψ_3 as the triad partners. Early in the sequence energy interchange must be small and interacting modes may be represented by the appropriate homogeneous solution of weakly time dependent amplitude, e.g.

$$\psi_1 = A_1(t) \sin m_1 x \sin n_1 z \cos \omega_1 t, \quad d^2A_1/dt^2 \ll A_1 \omega_1^2.$$

The interaction products forming the right-hand side of (18) are evaluated, viz.

$$[g/HJ(\psi_k, \rho_l)_x - J(\nabla^2\psi_k, \psi_l)_t]_{k,l=1,3}$$
$$= S_{13} A_1 A_3 \sin (m_1 + m_3)x \sin (n_1 + n_3)z \sin (\omega_1 + \omega_3)t + \text{other terms}, \quad (20)$$

where

$$S_{13} = \tfrac{1}{8}(m_1 n_3 - m_3 n_1)\,[(m_1^2 + n_1^2 - m_3^2 - n_3^2)\,(\omega_1 + \omega_3) + (m_1 + m_3)\,(m_1/\omega_1 - m_3/\omega_3)\Omega^2].$$

Equivalent expressions for S_{23} and S_{12} are found by substitution.

Say now that the part ψ_2 of ψ forced by the above interaction term has the form

$$\psi_2 = A_2(t) f_2(t) \sin m_2 x \sin n_2 z,$$

itself satisfying the tangentiality conditions at the container boundaries, then substitution in (18) gives, in part,

$$A_2 \left(\frac{d^2 f}{dt^2} + \frac{\Omega^2 m_2^2}{m_2^2 + n_2^2} f \right) = - S_{13} A_1 A_3 \sin (\omega_1 + \omega_3)t - 2 \frac{dA_2}{dt} \frac{df}{dt} (m_2^2 + n_2^2) \quad (21)$$

for those components for which $m_2 = m_1 + m_3$, $n_2 = n_1 + n_3$. However, if in satisfaction of the last of (19) the eigenvalue of the homogeneous equation $\omega_2^2 = \Omega^2 m_2^2/(m_2^2 + n_2^2) = (\omega_1 + \omega_3)^2$, then the right-hand side of (21) must vanish and

$$dA_2/dt = S_{13} A_1 A_3 / 2(m_2^2 + n_2^2)\omega_2 \quad (22)$$

and

$$f = \cos (\omega_1 + \omega_3)t.$$

Similarly,

$$dA_3/dt = S_{12} A_1 A_2 / 2(m_3^2 + n_3^2)\omega_3, \text{ etc.} \quad (23)$$

Mutual enhancement of the subliminal modes ψ_2, ψ_3 will occur if

$$S_{12} . S_{13}/\omega_2 \omega_3 > 0.$$

In the presence of viscosity, energy acquired by interaction is opposed by dissipation. Because of the orthogonality of the modes, the dissipation rate of each mode depends on its own amplitude, and, by analogy with (16), simultaneous equations for the evolution of amplitude may be written:

$$\left.\begin{aligned} (m_2^2 + n_2^2) \frac{dA_2}{dt} &= \frac{S_{13} A_1 A_3}{2\omega_2} - T_2 A_2, \\ (m_3^2 + n_3^2) \frac{dA_3}{dt} &= \frac{S_{12} A_1 A_2}{2\omega_3} - T_3 A_3, \end{aligned}\right\} \quad (24)$$

for the subliminal modes, and

$$(m_1^2+n_1^2)\frac{dA_1}{dt} = (m_1^2+n_1^2)\omega_1 b_1 \sin\phi_1 + \frac{S_{23}A_2A_3}{2\omega_1} - T_1A_1, \tag{25}$$

for the original, forced mode. For the initial stages A_2A_3 is small and, if A_1 has already acquired a terminal amplitude, equations (24) combine to predict a simultaneous exponential growth of A_2 and A_3 provided

$$A_1 = A_{1T} \geqslant A_{1c} \equiv 2(T_2T_3\omega_2\omega_3/S_{12}S_{13})^{\frac{1}{2}}. \tag{26}$$

It should be noted that the above formulation strictly applies when phase relationships between participating modes are defined only by the interaction. This is the case when L/H is such that (19) are *exactly* satisfied, but otherwise prevails only in the initial stages of growth of the subliminal modes. However, there is no immediate reason to question the validity of (26) in relation to the present experiments.

Clearly there is scope for further study of *damped* interaction particularly in relation to finite amplitude limit states for the participating modes and (in view of the plurality of triads of similar resonance L/H), behaviour off resonance, with or without more than one interacting triad. This is reserved for separate investigation.

3. Experiments

Experiments were performed in a 'Perspex' walled tank 1·83 m long, 0·23 m ($= B$) wide. One end was bounded by a paddle pivoting about a horizontal axis 0·163 m above the bottom plane, and sealed with felt around its edges. A movable vertical plate also sealed with felt formed the other end of a test section. The paddle could be oscillated through $\pm 0{\cdot}1$ rad by means of a disconnectable rod 0·54 m long, on a crank of adjustable stroke, turned via a gear box by an electronically controlled d.c. motor whose speed was regulated approximately $\pm 0{\cdot}2$ % to a level variable to 0·1 %.

The tank was filled with linear stably stratified common salt solutions created in a method similar to that proposed by Oster (1965), but in an apparatus capable of making exponentially stratified solutions in large volumes. A description will be given elsewhere. Stratifications so produced were linear within the limits of resolution of the measuring device, between 5 % of the total density difference for the weakest stratification, $\rho_0'/\rho = 1{\cdot}24\times10^{-2}\,\mathrm{m}^{-1}$, and 2 % for the strongest, $\rho_0'/\rho = 2{\cdot}9\times10^{-1}\,\mathrm{m}^{-1}$.

The tank was filled slowly from a retractable bottom mushroom opening where dye solution was injected at intervals to form sharp coloured layers throughout the depth. After filling, cetyl alcohol was deposited in solution with ether on the free surface to inhibit evaporation and the attendant convectively-mixed surface layer, and to further suppress conduction effects of 1·3 cm sheet of polystyrene was floated on the surface. The top surface was therefore virtually plane and rigid.

Stratifications would remain linear within a centimetre or so of top and bottom

for many days, though the dye was diffuse after a day. The confined depth H was 0·326 m in all tests.

Motions within the fluid were measured at a position ($\frac{1}{4}L, \frac{1}{2}B, \frac{11}{12}H$) where L is confined length, using a probe comprising a fine wire fork on a 2 mm tubular sting, bearing an S.T.C. type U23UD miniature thermistor bead. The probe assembly was spray coated with vinyl lacquer to prevent stray currents and electrolysis. Calibration was performed for each test by oscillating the probe in still water about its measuring position, in a near-horizontal arc of large radius, at the same frequency as the motion to be measured. The probe formed one arm of a d.c. constant-temperature bridge, and the output (variation in thermistor current) was monitored on a pen recorder. By varying the arc length, a range of equivalent horizontal oscillations was calibrated for each test. In comparison with directly measured particle movements the calibration was nearly logarithmic down to 2·5 mm/sec, and accuracy was good (about 1 %).

The phase of the motion relative to the paddle oscillation was determined by timing the interval between change in sign of the time derivative of thermistor bridge output (corresponding to a velocity minimum at the probe) and a fixed phase event in the paddle motion. This method, made necessary by the long oscillation periods involved, is vulnerable to aliasing and time-constant errors, but these were minimized by calibration procedure, and phase of minimum velocity was considered accurate to $\pm 2°$.

Visualizations were by unfocused shadowgraph using a tungsten source. Wave amplitudes measured on the shadowgraph screen, corrected for parallax, agreed closely with thermistor measurements.

3.1. *Steady resonant waves*

Experiments were confined mainly to a configuration where the $M = 2$, $N = 1$ mode (subsequently referred to as 2/1) and its harmonics ($2N/1N$, N odd) were forced near resonance. Contained lengths L were $2\sqrt{3}H$ and $3{\cdot}58\,L$ with resonant frequencies 0·5 Ω and 0·488 Ω respectively.

The procedure was to engage the rod on the paddle with the crank turning at present stroke and speed. When the recorded amplitude and phase appeared stable, either stroke or speed were changed to cover a range in α and ϕ. Each test was terminated by disengaging the rod and recording the decay in amplitude of the free oscillation.

The rate of decay in amplitude is increased slightly in the presence of the measuring probe and small asperities on the tank surface, the most important being bubbles accumulating on the polystyrene lid.

Probe and top dissipation could be corrected for by running decay tests with two probes, and without the top, in which state the cetyl alcohol film presented an almost-rigid top boundary.

In the range of internal velocities experienced, small bluff asperities were expected to exhibit a drag coefficient proportional to velocity to approximately the inverse half power (Hoerner 1953). Expressed as an addition to the rate at which a free oscillation will decay, the correction to T in (17) is

$$\Delta T \propto A^{\frac{3}{2}}\omega^{\frac{1}{2}}R^{-\frac{1}{2}}. \tag{27}$$

Since it was not practicable to perform interference tests in each experiment, results were corrected on the basis of the above formula, for which the constant of proportionality was determined from the results of a single test. Side and bottom asperities were not corrected for.

Figure 1 shows the decay in amplitude of a free mode $M/N = 2/1$,

$$L/H = 3{\cdot}58, \quad R = 6{\cdot}8 \times 10^4.$$

Amplitude is expressed in units of dimensionless stream function $Q = A/\omega H^2$ and is corrected for harmonic mode decay, using (17). Q is plotted against number of cycles after the cessation of forcing. R is based on the mean viscosity ν of the solution, variations in which were usually insignificant. The theoretical line drawn includes the correction term, (27). Agreement is very close. The apparent scatter in the results is caused by transient waves created by crank disengagement.

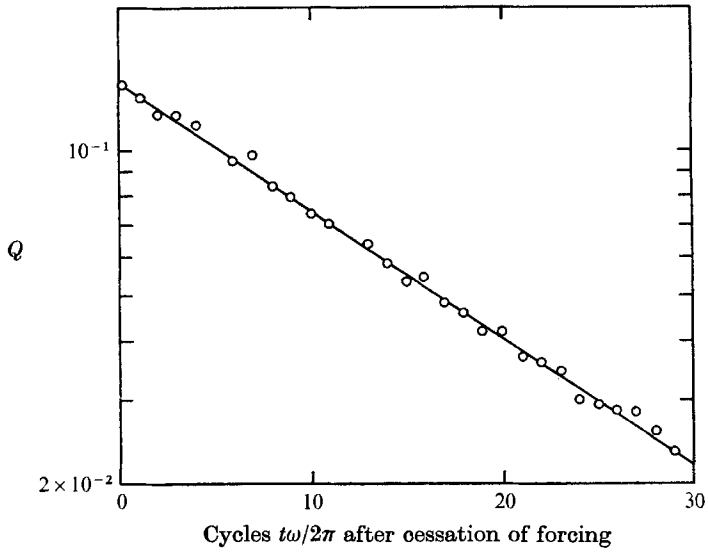

FIGURE 1. Decay in amplitude of a single free wave mode, $M = 2$, $N = 1$; $L = 3{\cdot}58\,H$, $H = 32{\cdot}6$ cm, $R = 6{\cdot}8 \times 10^4$. ○, experiment; —, theoretical, including correction for probe and top dissipation.

Figure 2 plots the mean decay constant per cycle of oscillation as a function of dissipation parameter R, compared with the theoretical prediction. Here it is the experimental points which have the above correction applied, since the amplitude range varied from test to test. Agreement is again close, with the apparent upward inflexion of the result at highest R being associated with the emergence of instability in the boundary layers, clearly visible in shadowgraphs.

In figure 3 the steady terminal amplitudes of oscillation, as measured by thermistor for numerous tests with $L = 2H\sqrt{3}$, are presented as an amplitude-phase locus. For presentation the amplitude is normalized using (16) with the theoretical value of G substituted. Agreement is satisfactory apart from an apparent phase error of about 10° occurring as the oscillation lead ahead of paddle motion becomes small.

Figure 4 gives amplitude and phase history for a single test during which the forcing frequency was changed several times. Frequency, as a fraction of the natural frequency given by (6), is marked on the figure. Also marked is the theoretical amplitude evolution computed using (16). The computed points are corrected for harmonic mode contribution, assuming constancy of phase relative to the fundamental.

The effect of phase error at low ϕ is clearly apparent, but otherwise (16) is adequate to describe the evolution.

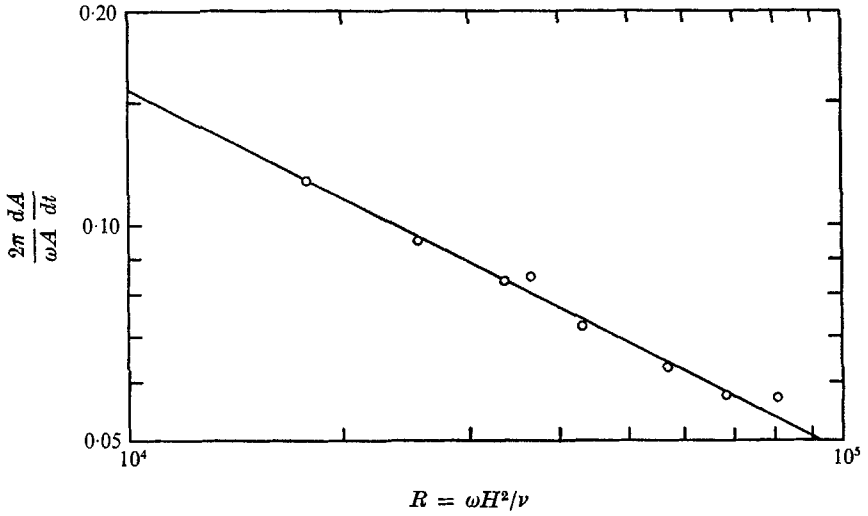

FIGURE 2. Dependence of decay rate on dissipation parameter R for a single free wave. ○, experiment, corrected for dissipation with top and probe; —, theoretical.

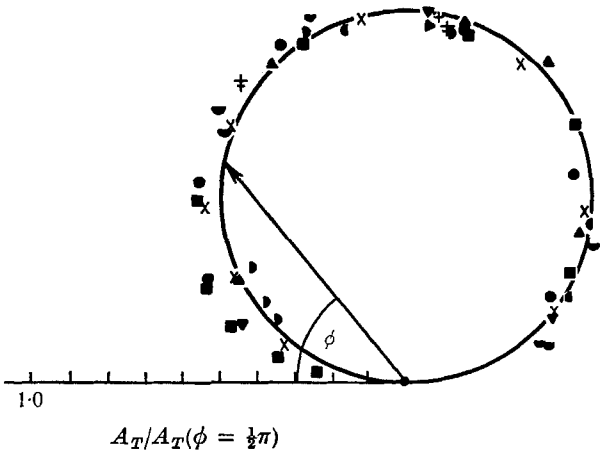

FIGURE 3. Amplitude-phase locus of a steady, continuously forced $M/N = 2/1$ mode. Theoretical line is from (16). ▲, ▼, $\Omega = 1{\cdot}43$ sec^{-1}; +, ∔, 0·305 sec^{-1}; ◗, ◖, ◒, 1·37 sec^{-1}; ×, ●, ■, 1·35 sec^{-1}; ▲, 0·483 sec^{-1}.

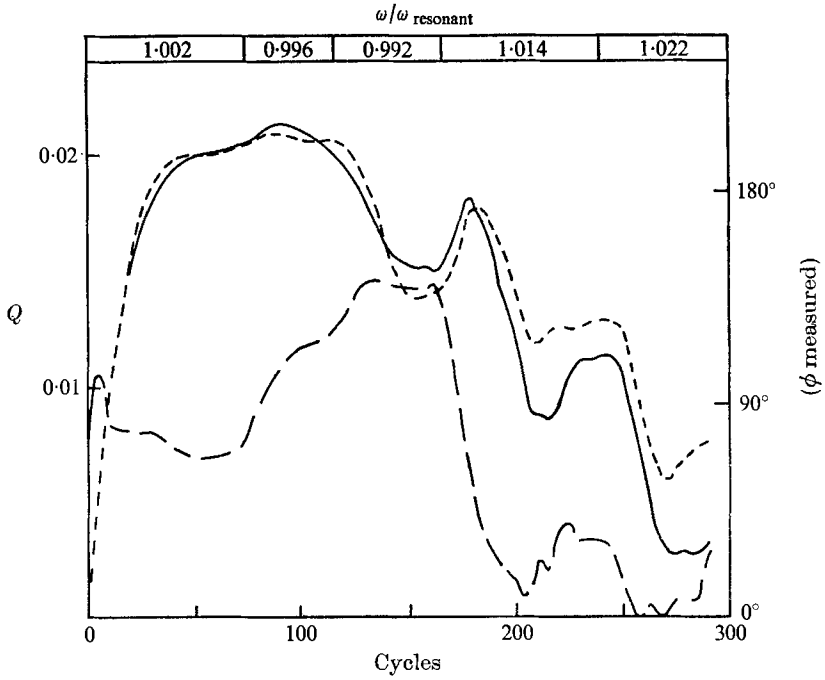

FIGURE 4. Amplitude and phase history for a continuously forced $M/N = 2/1$ mode. $\Omega = 2\omega_{\text{resonant}} = 1{\cdot}43\ \text{sec}^{-1}$, $R = 7{\cdot}15 \times 10^4$: – – –, measured amplitude; — —, measured phase, ϕ. —, calculated amplitude using (30) and measured phase. Forcing frequency ω as a fraction of resonant frequency is marked on top scale.

3.2. *Modes of resonant instability*

It was found in the execution of the steady-wave experiments that after the oscillation had been sustained for some time, the shadowgraph wave form, a indicated by the dyed layers, became increasingly modulated by other waves of frequency different from the forcing frequency. A precursor to this visible evidence appeared on the pen-traces of thermistor bridge output (which, because of the logarithmic response, was very sensitive to modulation of the *minimum* speed record). This was immediately followed by perceptible modulation of recorded maximum speed, and phase. Figure 5 (plate 1) is a photograph of the recorder trace and figure 6 (plate 2) a sequence of shadowgraphs, taken concurrently, of an $M/N = 2/1$ oscillation forced at $\alpha = 0{\cdot}031$; $\omega = 0{\cdot}499\,\Omega = 0{\cdot}65$ sec^{-1}. In figure 5 the co-ordinate scales are speed maximum and phase of minimum speed in advance of paddle motion minimum. Time is expressed in cycles after commencing excitation. The stages marked (*d*), (*e*) and (*f*) correspond with figures 6(*d*), (*e*) and (*f*). The symmetry of the wave distortion is striking. No true turbulence appeared during the test period and in these figures the motion remained completely two-dimensional over the interior region width.

Stronger forcing gave rise to more abrupt instability, frequently with a different combination of modulating waves. Figure 7 (plate 3) presents a sequence for similar conditions to those of figure 6 but with $\alpha = 0{\cdot}0575$. True turbulence, as viewed on the shadowgraph, had a characteristic vermiculate appearance and

was always preceded by the extensive formation of sharp density discontinuity layers, or 'traumata'. These appeared to arise from two separate kinds of disturbance. In the first, the isopycnic dyelines could be seen to be overturned with a subsequent collapse to produce a local gradient intensification. In the second, as common, kind there appeared to be no overturning, but the trauma first showed itself as a nearly vertical short line or collection of lines in a region where the principal compressive strain was near horizontal and large. Also present in such regions there frequently appeared diagonal radial lines aligned roughly in the planes of maximum shear rate. These vanished when the motion reversed and thus seemed not to be 'traumatic' to the stratification. The more pronounced diagonal lines on the right-hand side of figure 7(*d*) are an accumulation of the first kind of traumata and were possibly assisted to appear by characteristic rays of short internal waves from the wave maker, though the almost concurrent appearance on the left side of similar traumata suggested that the wave maker was not responsible for any pronounced asymmetries. The diagonal lines near the centre at the left of the same figure are those associated with the second kind of disturbance. The traumata seemed to be 'contagious', tending to spread in consecutive cycles of oscillation in groups around the original discontinuity.

The faint lines† at the right and left of figure 7(*c*) are evidently the result of a side wall boundary-layer instability. Similar cross flow 'roll waves' could be seen also on the end walls of the tank. There was nothing to suggest that these waves had any significant effect on the interior motion.

For a set of tests in which the tank length was held constant at $2H\sqrt{3}$ the forcing frequency ω was varied over a range resonantly exciting fundamental modes M/N from 1/1 to 5/1. The components of unstable modulation of each of these modes were then identified by finite Fourier analysis of dyeline photographs. This quantified the magnitude of waves of individual horizontal and vertical modal number at an arbitary time. In corroboration the measured period of modulation on the maxima and minimum of the speed-record traces, with equation (6), defined a finite set to which the dominant unstable modes belonged. Combined, these observations identified the unstable modes with a high degree of certainty.

Table 1 compares the modes predicted to comply most closely with (19)‡, and pairs of the strongest unstable modes identified experimentally. Without exception the latter, listed in order of frequency of occurrence, are members of the theoretically predicted triads. In addition to these, unforced $N = 1$ modes were usually present. To quote one example, for an $M/N = 2/1$ mode, weakly forced, the five largest vertical modal amplitudes at the instant of photographing were

$$M/N = 2/1{:}0{\cdot}074H; \quad 6/6{:}-0{\cdot}014H; \quad 4/5{:}-0{\cdot}009H;$$
$$6/1{:}0{\cdot}0089H; \quad 4/1{:}0{\cdot}0080H.$$

The tendency for the emergent unstable triads to differ under strong or weak main-mode forcing is worth noting. For strong 3/1 mode forcing the emergence

† Note added in proof: These are barely perceptible in the reduced figures, but appear as closely spaced lines in the right and left quarters, sloping downwards towards the outside.

‡ Predictions were based on the quality of the correspondence of $\omega_2+\omega_3$ with ω_1.

of 2/1 and 1/2 modes appeared to be associated with starting transients, and transients may have predetermined the interaction for other strongly forced tests. In the 3/1 case the interesting situation arose where those large wavelength unstable modes de-energized the forced mode without traumatic distortion occurring at any time, while with weaker forcing, giving rise to 6/4, 3/3 instability, distortion and turbulence could be precipitated.

In the case of the simplest (1/1) mode, forcing had to be strong before any irreversible distortion appeared, and even then the modulating modes could not be identified photographically. For this particular case the critical amplitude A_{1c} in (26) is complex, and there is therefore implicit confirmation that no unstable interaction should occur. Subsequent to the emergence of traumata, modulation having the predicted frequency appeared on the thermistor record. When traumata first appeared the dimensionless amplitude $Q = A/H^2\omega$ was 0·170.

Main wave mode ψ_1		Predicted unstable modes					Observed unstable modes	
M_1/N_1	ω_1/Ω	M_2/N_2	ω_2/Ω	M_3/N_3	ω_3/Ω	$(\omega_2+\omega_3)/\Omega$	M_2/N_2	M_3/N_3
1/1	0·277	4/7	0·163	3/8	0·108	0·975*	†	†
		4/9	0·127	5/10	0·143	0·974*	4/7	3/8‡
2/1	0·500	6/6	0·277	4/5	0·225	1·005	6/6	4/5
							or	
		5/4	0·339	3/5	0·171	1·020	5/4	3/5§
3/1	0·655	6/4	0·397	3/3	0·277	1·031	6/4	3/3
		2/1	0·500	1/2	0·143	0·982	and, or	
		8/6	0·359	5/5	0·277	0·972	2/1	1/2§
4/1	0·756	6/3	0·500	2/2	0·277	1·028	6/3	2/2
							or	
		8/4	0·500	4/5	0·225	0·959	8·4	4/5
5/1	0·822	8/3	0·610	3/4	0·212	1·000	7/3	2/2
		7/3	0·559	2/2	0·277	1·017		

TABLE 1. Comparison of closest theoretical unstable modes, with those observed. * $(S_{12}.S_{13}/\omega_2\omega_{23}) < 0$; see text. † Turbulent degeneration. ‡ Implied from recorded trace periodicity. § Strong forcing of main wave.

Except in this last example, the primary instability was recognizably interactive, and the unstable modes identified all possessed a frequency less than that of the forced mode, confirming Hasselmann's (1967) prediction.

If forcing was sustained at a supercritical level the distortion of the wave profile became increasingly complex, till the primary modulations were unrecognizable, though (excepting the 3/1, 2/1, 1/2 interaction) the forced mode was still dominant. The intensity of the modulation waxed and waned but there was no evidence that the unstable modes were interacting to re-energize the forced mode.

Except when forced to a level where intense true turbulence occurred, the density stratification appeared to have suffered very little modification after the motion had been allowed to decay. There was shadowgraph evidence that, on some occasions, local intensification of the density gradient had occurred at

several levels throughout the depth, but such steps were too weak to be resolved by conductivity sounding. When turbulence had been forced for a protracted period the density gradient was slightly weakened, most notably near the top and bottom boundaries.

3.3. *Quantitative limits to instability of a* 2/1 *mode*

To test quantitatively the predictions of § 2.3 a container geometry of

$$L/H = 3{\cdot}58$$

was used, for which the triad $M/N = 2/1,\ 6/6,\ 4/5$ closely satisfies (19). In view of the long testing times involved, there was only one practical technique in finding the limiting amplitude A_{1c} for the forced 2/1 mode at the onset of instability. This was to force the mode to a supercritical level and then, by reducing

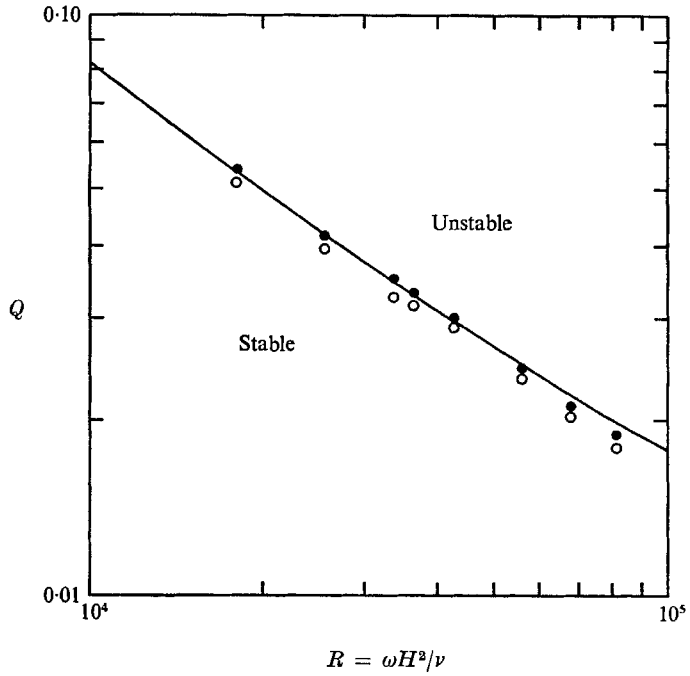

FIGURE 8. Amplitude threshold for interactive instability of a $M/N = 2/1$ oscillation, as a function of dissipation parameter R. Theoretical: —, given by (26). Experiment: ●, degenerate 6/6 and 4/5 mode oscillation could be sustained at a detectable level; ○, degenerate modes would not be sustained without increasing main mode amplitude.

the stroke of the paddle, lower the amplitude gradually till the unstable modes could not be sustained at a level perceptible on the thermistor pen record. As mentioned earlier, the minimum velocity recorded is very sensitive to superimposed motion. By this means A_{1c} was found for a number of tests with different density gradient (and hence R), within very close limits.

Figure 8 presents the results in comparison with the theoretical prediction derived from (26), frequencies being defined according to the fourth of (19), and T_2 and T_3 obtained using a value of G determined from the sum of internal and

boundary dissipation (12) and (13), but *excluding* probe dissipation. On this figure the solid points represent the lowest levels at which the modulating waves could be sustained, and the open points are the highest levels when they were not.

Agreement with the analytic prediction is remarkably good over the whole experimental range, and testifies to the adequacy of the formulation of the interaction equations, and of the method of estimating dissipation. Evidently the assumption of linear independence between the modes is justified, as the presence of non-cancelling interactions would contribute greatly to boundary-layer dissipation. Neglect of the non-linear probe dissipation terms in T_2' and T_3', which vanish more rapidly than A_2 and A_3, is also justified.

As a matter of procedural simplicity the results presented in figure 8 were all obtained with the forcing frequency adjusted to maintain the maximum energization rate ($\phi \approx 90°$). Nothing in the experiments suggested that ϕ influenced A_{1c} to an appreciable degree, and symmetry of the observed waveforms suggested that wave maker induced asymmetries were insignificant.

4. Critical conditions for wave breaking

These experiments were initially intended to provide a well-defined internal wave field, for the purpose of testing kinematical criteria for the 'breaking' of such waves. It has succeeded instead in showing the importance of interactive instability, but the original purpose should not be forgotten.

On the basis of the visible sequence of events it would appear, in the initial stages of the interactive instability, that apart from weak viscous effects no irreversible 'traumatic' distortion necessarily occurs. The discrete and abrupt appearance of density-discontinuity traumata at a second stage suggests that in combination, the forced mode and its parasites do eventually exceed some kinematic conditions in *localized regions*. These regions then become more numerous because the traumata produced contribute to the kinematic distortion elsewhere. Evidence for this is the tendency for the traumata to spread most rapidly along directions at the characteristic angles $\pm \arctan |m/n|$.

The next stage in the breaking process is the creation of 'true' turbulence which evidently results from the complex distortions *induced* by the traumata. The most that should be stated in describing this stage is that, as viscosity vanishes in importance, turbulence must inevitably follow the appearance of the traumata.

It is up to the second stage that hope remains of being able to calculate the critical kinematical conditions. The present experiment generally proves inappropriate because a multiplicity of modes of changing strength makes description of the motion field very difficult. (Experiments are presently in progress using a more suitable configuration.) An exception however, is the 1/1 mode, for $L/H = 2\sqrt{3}$, which 'broke' without interactive instability. As a matter of interest the magnitudes of some of the potentially important parameters were calculated, using the first-order steady-field description,† (8), for the fundamental mode and its first three harmonics, and (5) (to define harmonic phase relationship), (12), (13) and (17).

† Accurate to second order in Q (Thorpe 1968).

From pen records and photographs, the dimensionless amplitude Q_1 of the fundamental mode immediately prior to the appearance of traumata, was 0·170. Estimated harmonic mode amplitudes were

$$Q_3, \quad 1{\cdot}95 \times 10^{-3},$$
$$Q_5, \quad 2{\cdot}17 \times 10^{-4},$$
$$Q_7, \quad 4{\cdot}9 \times 10^{-5}.$$

The gross Richardson number Ri defined as $(\Omega/\text{peak vorticity})^2$, i.e.

$$Ri = \Omega^2\{\omega \sum_{N=1,3,5,7} Q_N k(N) N^2 (m_1^2 + n_1^2)\}^{-2},$$

was 4·72, where $k = (-1)^{(N-1)/2}$. The maximum isopycnic surface slope $\hat{\theta}$, occurring at $(\frac{1}{2}L, y, \frac{1}{2}H)$ and given by

$$\hat{\theta} = \arctan\left[\frac{\Sigma_1}{(\Sigma_1 \Sigma_2)^{\frac{1}{2}}} \tan (\Sigma_1 \Sigma_2)^{\frac{1}{2}}\right],$$

was 7·8°, agreeing well with photographs. Here

$$\Sigma_1 = \sum_{N=1,3,5,7} Q_N N^2 m_1^2 k, \quad \text{and} \quad \Sigma_2 = \sum_{N=1,3,5,7} Q_N N^2 n_1^2 k.$$

The internal Froude number, defined as $F_i = (\hat{U}/\omega H)^2$ where $\hat{U}$ is maximum horizontal velocity, was 0·31. Evidently, neither Ri, $\hat{\theta}$ nor F_i approach values that are critical in other, better-understood situations. Ri would be lowered slightly if based on local $(\frac{1}{2}L, y, \frac{1}{2}H)$ *dynamic* vertical density gradient ρ_z, but since $\hat{\theta}$ is only 7·8° the effect must be small.

Thus the question of which, if any, of the above parameters is important remains unresolved, the difficulty being that all, in the present context, depend on a single quantity Q_1.

5. Conclusion

The present work has shown the existence of a limit to the amplitude of a steadily forced standing internal gravity wave in a fully bounded continuously stratified fluid, beyond which it will suffer a progressive and destructive distortion of form. Provided forcing is not too vigorous, the process *primarily* responsible is a resonant-interactive instability in which pairs of initially subliminal free wave modes are selectively amplified. With rectangular boundary geometry, the interacting modes are uniquely defined by the ratio of container length to depth, and if $\omega H^2/\nu$ is high, analytic description is simple and accurate. This has permitted an experimental verification of resonant-interaction theory quantitatively more accurate than in other previously published studies.

It has been found experimentally that a two-dimensional wave may suffer considerable distortion without the emergence of cross oscillation. If the net motion induced by the forced wave and its modulating modes is sufficiently large, traumatic distortion of the density field occurs in the form of localized regions of sharply increased density gradient. This evidently precedes the appearance of

true turbulence. Kinematic conditions leading to traumatic distortion seem to be realized more easily in the presence of interactive instability, but the present experiments were unsuitable for resolving these conditions.

This work was done as a guest of the C.S.I.R.O. during the tenure of a Queen Elizabeth II Research Fellowship. Acknowledgement is gratefully given. Thanks are also due to Drs F. K. Ball and R. Smith for their comments on the manuscript.

REFERENCES

ALDRIDGE, K. D. & TOOMRE, A. 1969 *J. Fluid Mech.* **37**, 307.
BAINES, P. G. 1967 *J. Fluid Mech.* **30**, 533.
BENJAMIN, T. B. & FIER, J. E. 1967 *J. Fluid Mech.* **27**, 417.
CRAIK, A. D. D. 1968 *J. Fluid Mech.* **34**, 531.
DAVIS, R. E. & ACRIVOS, A. 1967 *J. Fluid Mech.* **30**, 723.
HASSELMANN, K. 1967 *J. Fluid Mech.* **30**, 737.
HOERNER, S. F. 1953 *Fluid Dynamic Drag*. Hoerner.
MALKUS, W. V. R. 1968 *Science*, **160**, 259.
MARTIN, S., SIMMONS, W. F. & WUNSCH, C. I. 1969 *Nature*, **224**, 1014.
MCEWAN, A. D. 1970 *J. Fluid Mech.* **40**, 603.
MCGOLDRICK, L. F. 1970 *J. Fluid Mech.* **40**, 251.
OSTER, G. 1965 *Scient. Amer.* **213**, 70.
TAYLOR, G. I. 1953 *Proc. Roy. Soc.* A **218**, 44.
THORPE, S. A. 1966 *J. Fluid Mech.* **24**, 737.
THORPE, S. A. 1968 *J. Fluid Mech.* **32**, 489.

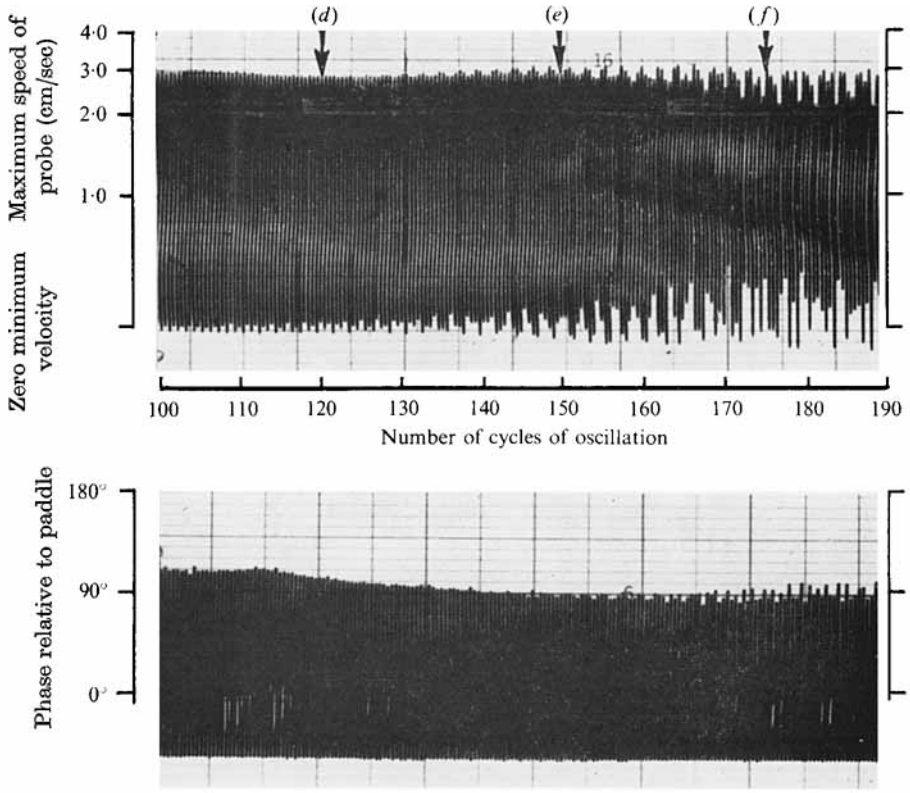

FIGURE 5. Photocopy of amplitude and phase records for $M/N = 2/1$ oscillation forced at $\alpha = 0{\cdot}031$; $\omega_1 = 0{\cdot}499\ \Omega = 0{\cdot}65\ \text{sec}^{-1}$. Photos in figure 6(*d*), (*e*) and (*f*) were taken at the positions marked. Time is expressed in cycles of oscillation after commencement of forcing.

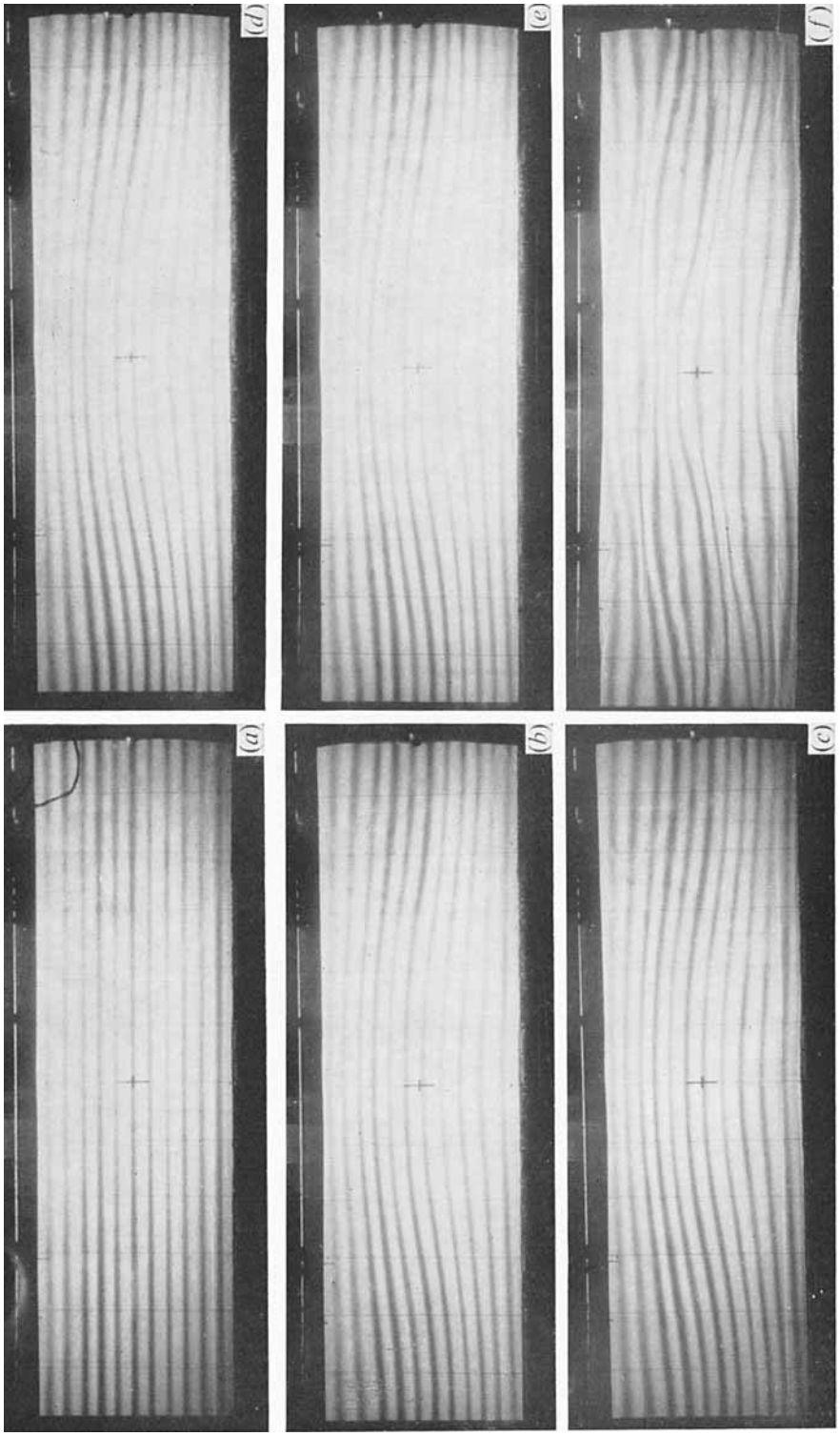

FIGURE 6. Shadowgraphs of wave evolution under conditions given for figure 5: (*a*) before oscillation; (*b*) 40 cycles; (*c*) 80 cycles; (*d*) 120 cycles; (*e*) 150 cycles; (*f*) 176 cycles.

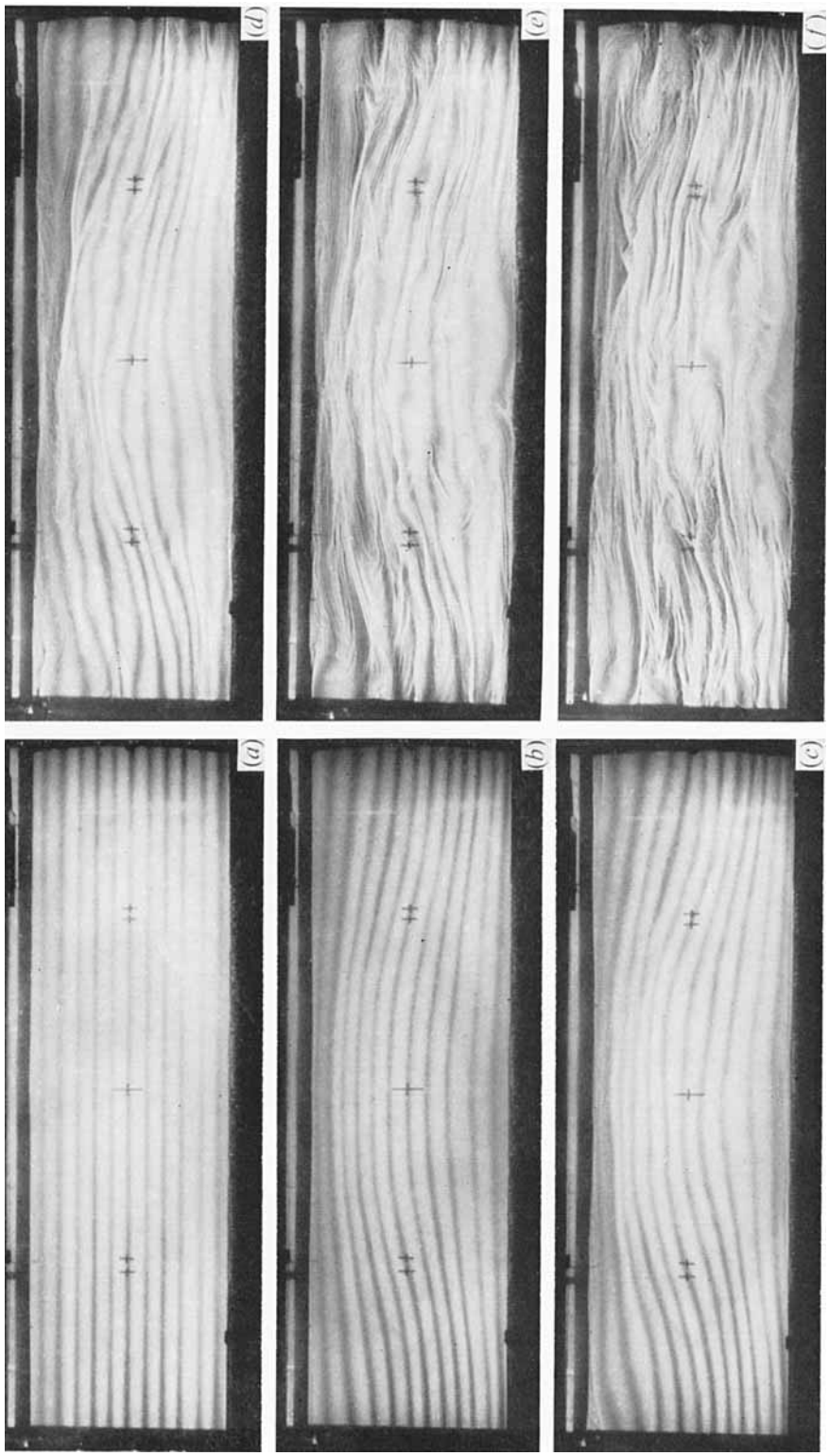

FIGURE 7. Shadowgraphs of wave evolution $M/N = 2/1$; $\omega = 0{\cdot}5\ \Omega = 0{\cdot}704\ \text{sec}^{-1}$; $\alpha = 0{\cdot}0568$: (*a*) before start, (*b*) 20 cycles; (*c*) 45 cycles; (*d*) 55 cycles; (*e*) 60 cycles; (*f*) 65 cycles.